

Eddy Currents Signatures Classification by Using Time Series: a System Modeling Approach

Blaise Guépie¹, Mihaly Petreczky², and Stéphane Lecoeuche³

^{1,2,3} *Mines Douai, IA, F-59508 Douai, France*

blaise.guepie@mines-douai.fr

mihaly.petreczky@mines-douai.fr

stephane.lecoeuuche@mines-douai.fr

ABSTRACT

Non destructive testing methods are often used in order to detect and classify structural flaws. The detection of structural flaws is useful for maintenance. In this paper we propose to classify flaws in ferromagnetic materials by measuring Eddy currents. Our approach consists of two steps. First, we use a system identification algorithm to find a dynamical system which describes the data. Then, we use the parameters of this dynamical system as a feature vector and we use support vector machines in order to classify the various cracks. We test our method on a well-known benchmark.

1. INTRODUCTION AND MOTIVATION

Non destructive testing methods are used for checking the presence of structural flaws (cracks, deformations, etc.) of materials without causing damage. This is useful for predictive maintenance. The most important methods for non-destructive detection of structural flaws are the following: ultrasonic (Cantrell & Yost, 2001), acoustic emission (Madaras, Prosser, & Gorman, 2005), terahertz ray (Němec, Kužel, Garet, & Duvillearet, 2004), X-ray (Elaqra, Godin, Peix, R'Mili, & Fantozzi, 2007), thermal (Clark, McCann, & Forde, 2003), optical method (Jie, Siwei, Qingyong, Hanqing, & Shengwei, 2009) and eddy currents (EC) (Smid, Docekal, & Kreidl, 2005).

In this paper, we propose using Eddy currents for detecting flaws. Methods based on measuring Eddy currents are popular, because measuring Eddy currents is cheap and it allows detecting clogged defects and to classify cracks. For any classification method, feature extraction is one of the critical steps. For Eddy currents, several feature extraction methods exist in the literature. (Jo & Lee, 2009; Song & Shin, 2000; Liu et al., 2013) use maximum amplitude and phase angle or

width of defect signal; (Oukhellou, Aknin, & Perrin, 1999; Smid et al., 2005) focus on the Fourier or wavelets transform parameters; (Lingvall & Stepinski, 2000; Ye et al., 2009) use principal component analysis or its kernel version.

In comparison to the existing methods for feature extraction, the main novelty of the proposed method lies in using parameters of dynamical systems as feature. This represents a novel application of system identification techniques to fault detection and health monitoring of ferromagnetic materials based on Eddy currents.

Our approach is based on two steps. First, using the measured data, we find a parametric dynamical model. This model represents current impedance values of eddy currents as function of past impedance values. We use a system identification algorithm for identifying the model parameters based on measured data. Thus, the obtained parameters serve as feature. We assume that each flaw corresponds to an unique parameter vector. We then use support vector machines to compute a classifier on the extracted parameter space.

The experimental evaluation shows that our approach gives good results.

The paper is organized as follows. Section 2 is devoted to the problem statement. Section 3 presents the data pre-processing step including denoising and re-sampling. A new method of feature extraction based on dynamical systems identification is explained in Section 4. The Support Vector Machines operating is briefly described in Section 5. Section 6 shows an example of classification of flaws using Eddy currents. Some conclusions are drawn in Section 7.

2. PROBLEM DEFINITION

Eddy currents are used in many applications of non destructive testing. When a conductive material is within a time-variable magnetic field created by a coil subjected to an alternative current, induced Eddy currents are developed inside the material without altering its characteristics. When an in-

Blaise Guépie et al. This is an open-access article distributed under the terms of the Creative Commons Attribution 3.0 United States License, which permits unrestricted use, distribution, and reproduction in any medium, provided the original author and source are credited.

homogeneity, a change in geometry or a flaw is present in the material, variations in the phase and magnitude of these eddy currents can be monitored, as they lead to a change of the coil impedance. This is the principle of material inspection by Eddy currents. Sensors travel across the surface of the material and the variations of the coil impedance are acquired and compared with an impedance reference. Then, in presence of a crack, the impedance data varies as function of sensor or material displacement, following a trajectory into a complex plane where abscissa is the resistance and the reactance is the ordinate.

By firstly considering aluminum structures, the goal of the method presented in this paper is to propose to automatically classify the type of defaults or cracks using as input the impedance data trajectory. To present the method, an existing database¹ composed of Eddy currents signatures from aluminum aircraft structures has been used. The database is composed of twelve types of crack, characterized by both penetration angle into the material and depth of penetration. Figure 1 shows characteristics of all the twelve cracks. For example, the first crack type is defined by 1.5mm of depth and 90° of penetration angle.

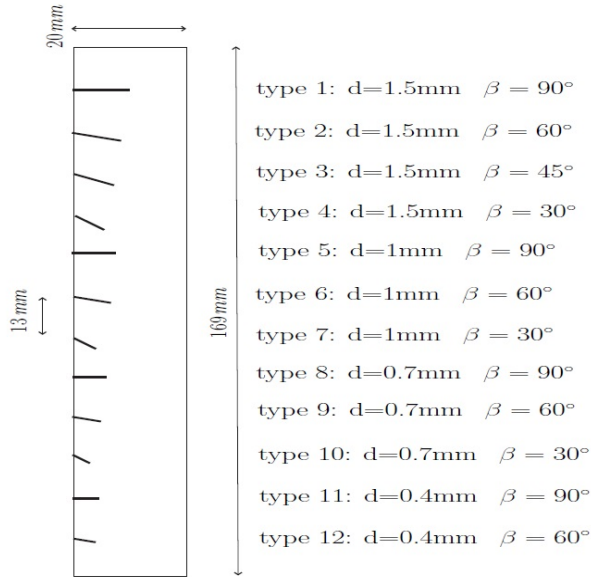


Figure 1. Aluminum sample with machined notches of different penetration angles and depths.

For each crack, acquired impedance data are complex discrete time series

$$\tilde{z}(k) = \tilde{x}(k) + j\tilde{y}(k),$$

where the resistance curve $\tilde{x}(k)$ and the reactance curve $\tilde{y}(k)$ are known. Each type of crack is scanned 20 times by a coil. This leads to 20 impedance trajectories. Figure 2 illustrates

different impedance trajectories for several types of crack.

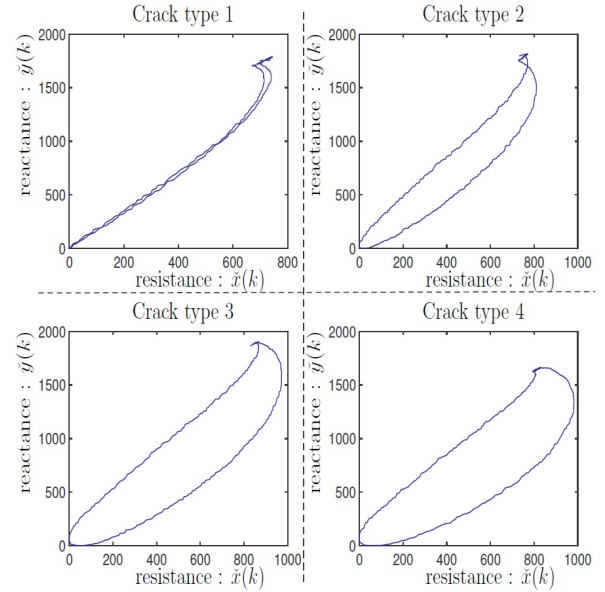


Figure 2. Impedance trajectories of four crack types.

The originality of this paper lies in classifying crack types using the parameters of temporal models that fit the impedance trajectories. Each component of the trajectory (resistance and reactance) will be considered as time series ARX model where its parameters will be used to classify the crack type. So, the main steps of the proposed method are :

- from each inspection, extract sequences $\tilde{x}(k)$ and $\tilde{y}(k)$,
- estimate θ_x and θ_y the parameters associated to the time series models,
- knowing the set of θ_x and θ_y , corresponding to the whole inspection database, build the classifiers.

Before explaining in detail the estimation and the classification steps, it is worth introducing remarks on the data preprocessing step.

3. DATA PREPROCESSING

First, in order to reduce noise impact, resistance \tilde{x} and reactance \tilde{y} are filtered. A standard median filter is used. For $k \geq 1$, the median values

$\tilde{x}(k)$ of $\{\tilde{x}(k - L_x + 1), \dots, \tilde{x}(k + L_x - 1)\}$ and $\tilde{y}(k)$ of $\{\tilde{y}(k - L_y + 1), \dots, \tilde{y}(k + L_y - 1)\}$ respectively replace $\tilde{x}(k)$ and $\tilde{y}(k)$ where $2L_x - 1$ and $2L_y - 1$ are the prescribed length of the median filter window.

Moreover, collected data come from a manual scanning. This implies that the scan speed varies over time and variations impact the impedance curve shape for the same crack. To reduce the effect of variate scanning speed, data $\{\tilde{x}(k)\}_{k=1}^M$ and $\{\tilde{y}(k)\}_{k=1}^M$ are re-sampled in order to get the same number

¹freely available on the website : <http://wireless.feld.cvut.cz/diagnolab/node/16>

of points for each crack. These filtered and re-sampled data $\{\hat{x}(k)\}_{k=1}^N$ and $\{\hat{y}(k)\}_{k=1}^N$ will serve as the second learning dataset.

Each type of cracks is characterized by the following two properties: “depth” and “angle”. Depth refers to the depth of the crack, and angle refers to the angle formed by the crack and the horizontal axis. That is, each crack is identified with a pair of numbers $(depth, angle)$, where $depth$ denotes the depth of the crack and $angle$ denotes the angle of the crack. Hence, we can classify cracks as follows. First, we construct a classifier which determines the angle associated with each crack based on measurement data. In this way, we obtain several groups of cracks, each group representing cracks with the same angle. Second, for each angle α , we construct a classifier which determines the depth of a crack whose angle equals α . This classifier will use measurements to determine the depth. Note that the second classifier is supposed to distinguish only cracks with the same angle. Figure 3 shows curves of impedance values for cracks with 60° of angle and $1.5mm$, $1mm$, $0.7mm$, $0.4mm$ of penetration depths. Each curve is a finite collection $\{(\hat{x}(k), \hat{y}(k))\}_{k=1}^N$ of data points, where $\hat{x}(k)$ is the real part and $\hat{y}(k)$ is the complex part of $\hat{z}(k)$, the filtered and re-sampled impedance value measured at time step k . It can be seen from the data that the shapes of the four cracks are similar but some are larger than other. Therefore, we can assume that the depth does not have impact on the shape of the curve except its magnitude. For this reason, we will apply a normalization step in order to find crack angles. That is to say, before computing the first classifier, we will divide the data points by a constant. Thus, the first dataset is composed of

$$\{(x(k), y(k))\}_{k=1}^N = \left\{ \frac{(\hat{x}(k), \hat{y}(k))}{\max_{k \in \{1, \dots, N\}} \sqrt{\hat{x}^2(k) + \hat{y}^2(k)}} \right\}_{k=1}^N$$

. Note that for the computation of the second classifier, we will use the original data points $\{(\hat{x}(k), \hat{y}(k))\}_{k=1}^N$, since the crack’s depth influences the magnitude of the data points and thus normalization could lead to loss of information.

4. FEATURE EXTRACTION BASED ON DYNAMICAL SYSTEMS

As we have seen before, each crack observation is composed of time series data points arising from Eddy currents measurements. It can be represented as curve in the complex plane, since each impedance value is a complex number. However, such a representation discards the temporal dependence between various data points. For this reason, in order to compute classifiers, we will use the time series $\{x(k)\}_{k=1}^N$ and $\{y(k)\}_{k=1}^N$. We will use these time series to compute a dynamical system whose input-output behavior is consistent with them. We assume that each group of flaws (i.e, each angle

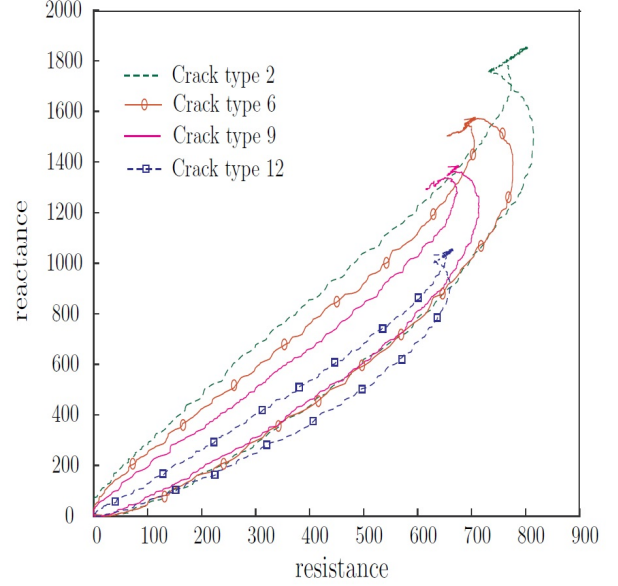


Figure 3. Cracks with 60° of angle and four penetration depths.

of penetration) determines an unique pair of parameters vectors, where each parameters vector corresponds to a dynamical system. It is worth noting that each pair of parameters vectors is extracted from one crack observation. Thus, parameters vectors are independent from each other. The first dynamical system models the resistance:

$$x(k) = \theta_x^T \phi_x(k) + \xi_x(k), \quad (1)$$

and the second one models the reactance:

$$y(k) = \theta_y^T \phi_y(k) + \xi_y(k), \quad (2)$$

where

$\phi_x(k) = [x(k-1), \dots, x(k-n_{a_x}), y(k-1), \dots, y(k-n_{b_x}), 1]^T$,
 $\phi_y(k) = [y(k-1), \dots, y(k-n_{a_y}), x(k-1), \dots, x(k-n_{b_y}), 1]^T$,
 (n_{a_x}, n_{b_x}) and (n_{a_y}, n_{b_y}) are models orders, $\{\xi_x(k)\}_{k \geq 1}$,
 $\{\xi_y(k)\}_{k \geq 1}$ are independent identically distributed random sequences and θ_x, θ_y are the associated parameters vectors.

We assume that for each crack, the pair of parameters vectors (θ_x, θ_y) determine the angle of the crack. More precisely, we assume that these pairs are close when cracks belong to the same group, i.e, the penetration angle is the same.

In this paper, we will use the *Recursive Least-Squares method* (abbreviated by *RLS*) as linear system identification algorithm because its recursive form is exact comparatively to the Least Mean Squares (LMS) and then, it converges more quickly to the solution. The RLS algorithm was proposed to determine the parameter θ of the equation

$$w(k) = \theta^T \psi(k) + \xi(k) \quad (3)$$

from finitely many measurements $\{w(k), \psi(k)\}_{k=1}^N$. Note that both (1) and (2) are of the form (3) with a suitable choice of $\theta(k)$, $\psi(k)$, $\xi(k)$ and $w(k)$. Below we describe the RLS algorithm. We will follow the presentation of (Ljung & Söderström, 1983). Let I be the identity matrix and let $P(0) = \sigma I$ be the initial auto-correlation matrix of data. For each new observation $(w(k), \psi(k))$, the update of $(\hat{\theta}^T(k-1), P(k-1))$ is given by:

$$\begin{aligned} \xi(k) &= w(k) - \hat{\theta}^T(k-1)\psi(k), \\ \hat{\theta}(k) &= \hat{\theta}(k-1) + \frac{\xi(k)P(k-1)\psi(k)}{\alpha + \psi(k)^T P(k-1)\psi(k)}, \\ P(k) &= \alpha^{-1}P(k-1) \left[I - \frac{\psi(k)\psi(k)^T P(k-1)}{\alpha + \psi(k)^T P(k-1)\psi(k)} \right] \end{aligned} \quad (4)$$

where $\alpha \in [0, 1]$ is the forgetting factor.

5. CLASSIFICATION OF CRACKS

The goal of this part is to identify the class membership of each crack. The classification is in two step. The first one is for discriminating the penetration angle into the material and the second one is for selecting the penetration depth. Several methods exist in classification theory. For labeled data, the Support Vector Machines (SVM) developed in (Vapnik, 2000) achieve excellent performance according to (Caruana & Niculescu-Mizil, 2006; Khelil, Boudraa, Kechida, & Draï, 2005). The following lines briefly explain SVM principle.

5.1. Two classes SVM

The SVM has been firstly used to separate two classes. Its principle is to maximize the separation margin ; the margin being the distance between the closest observations and the separator.

Consider a given training set $\{x_k, y_k\}_{1 \leq k \leq N}$ where the observation $x_k \in \mathbb{R}$ and the class variable $y_k \in \{-1, 1\}$. Suppose that data are linearly separable, i.e, there exists a linear classifier (w, b) such as

$$\begin{cases} w^T x_k + b \geq +1 & \text{if } y_k = +1 \\ w^T x_k + b \leq -1 & \text{if } y_k = -1 \end{cases} \quad (5)$$

The problem of finding the separator which maximizes the margin is equivalent to :

$$\begin{aligned} \min_{w,b} & \quad \frac{1}{2} \langle w, w \rangle \\ \text{constraint to} & \quad y_k(w^T x_k + b) > 1, 1 \leq k \leq N, \end{aligned} \quad (6)$$

where $\langle \cdot, \cdot \rangle$ is the dot product.

Generally, data are not separable. In this case, the margin of some observations are allowed to be less than one. Slacks

variables $\epsilon_k \geq 0$, $1 \leq k \leq N$ are introduced in order to solve the problem. The optimization problem becomes

$$\begin{aligned} \min_{w,b,\epsilon_k} & \quad \frac{1}{2} \langle w, w \rangle + C \sum_{k=1}^N \epsilon_k \\ \text{such that} & \quad \begin{cases} y_k(w^T x_k + b) > 1 - \epsilon_k \\ \epsilon_k \geq 0 \end{cases} \quad \text{for } 1 \leq k \leq N, \end{aligned} \quad (7)$$

where C is a positive real constant for determining the tolerance of the SVM to the poorly separated observations. The solution are $w = \sum_{k=1}^N \gamma_k y_k x_k$ and $b = b_0$ where $\gamma_k \geq 0$ for $1 \leq k \leq N$ and b_0 are obtained by solving the dual formulation of (7). Then, the decision function is

$$f(x) = \text{sign} \left(\sum_{k=1}^N \gamma_k y_k \langle x_k, x \rangle + b_0 \right). \quad (8)$$

When datasets are linearly non-separable, the trick is to project them on a high-dimensional feature space by using a nonlinear map $\psi(\cdot)$ such as the projections are linearly separable. Thanks to the Mercer's condition (Mercer, 1909), the calculation of the dot product $\langle \psi(x_{k'}), \psi(x_k) \rangle$ which often requires a lot of computational resources is replaced by the calculation of the kernel $K(x_{k'}, x_k)$. Two kernels are widely used: the Gaussian kernel $K(x_{k'}, x_k) = \exp\left(-\frac{\|x_{k'} - x_k\|^2}{2\sigma^2}\right)$ and the homogenous polynomial kernel $K(x_{k'}, x_k) = \langle x_{k'}, x_k \rangle^d$, where σ and d are tuning parameters.

In this paper, these parameters are selected as those minimize the leave-one-out cross validation error whose the procedure consists of:

- splitting the data set of size k into k smaller subsets
- a model is trained using $k-1$ subsets as training data
- the resulting model is validated on the remaining subset
- the previous both lines are repeated k times.

After using a kernel, the decision function (8) becomes

$$f(x) = \text{sign} \left(\sum_{k=1}^N \gamma_k y_k K(x_k, x) + b_0 \right). \quad (9)$$

5.2. Multi-class SVM

The mutli-class SVM is an extended version of two classes SVM. Here, it is supposed that the number of classes is greater than two.

Here, the One Against One SVM is used for classifying more than two classes. This approach is very intuitive. It consists of making several classifiers in order to compare pairs classes.

Thus, for classifying a dataset between M classes, we need to make $\frac{M(M-1)}{2}$ separators (Moreira & Mayoraz, 1998). A majority vote across the classifiers is applied to classify a new observation.

In brief, the global crack classification procedure is given by algorithm 1.

6. EXPERIMENTAL RESULTS

In order to test the reliability of our method, a database² composed of Eddy currents signatures from aluminum aircraft structures is used. In this database, there are twelve types of crack. Each type of crack is characterized by the angle and the penetration depth, is recorded 20 times. Figure 1 shows characteristics of all the twelve cracks.

The first classification task is devoted to the penetration angle. Four groups are created from the twelve types of crack. The first group contains 80 cracks with 90° of angle and 1.5, 1, 0.7, 0.4 mm of penetration depth. The second group contains 80 cracks with 60° of angle and 1.5, 1, 0.7, 0.4 mm of penetration depth. In the third group, there are 20 cracks with 45° of angle and 1.5 mm of penetration depth. The last group contains 60 cracks with 30° of angle and 1.5, 1, 0.7 mm of penetration depth.

The parameters used in the first part of classification algorithm (see algorithm 1) are the following. The median filters widows size are $L_x = 30$ observations and $L_y = 30$ observations. The fixed number of observations is $N = 300$. The re-sampling factor is $factor = N/M$ where M is the curve number of observations. The Recursive Least Squares forgetting factor is $\alpha = 9.99 \times 10^{-1}$, its value for the initial auto-correlation matrix is $\sigma = 10$ and its initial parameters $\theta_x(0), \theta_y(0)$ are randomly selected.

Each crack observation is composed of time series data points arising from Eddy currents measurements. For discriminating different cracks, our procedure consists to extract representative parameters vector from each crack observations. The extracted parameters vectors are independent from each over. Several values of order are tested for both dynamical systems identification (1) and (2) in order to select the model parameters. The values which minimize the least squares errors are $(n_{a_x}, n_{b_x}) = (0, 2)$ and $(n_{a_y}, n_{b_y}) = (0, 2)$. Figure 4 shows estimations of measured resistance and reactance. Both estimated curves obtained from two order dynamical systems are close to real curves.

It is worth nothing that the goal of our extracted parameters is not exactly to predict the real curves of resistance and reactance. The goal of prediction is to evaluate whether the extracted parameters vector explains the dynamic of the considered time series. The evaluation step allows defining the

Algorithm 1 Procedure of cracks classification

- 1: Have Eddy currents measuring data
- 2: Removal of edge data: a set of uninformative data (null data) to the right of each curve is deleted
- 3: Data filtering: set the windows sizes L_x and L_y of median filters
- 4: Duplication of the dataset $\{(\hat{x}(k), \hat{y}(k))\}_{k=1}^M$: the 1st dataset will be processed for discriminating angle and the 2nd dataset will be used for discriminating depth without further processing
- 5: Re-sampling of resistance and reactance curves extracted from the 1st dataset: set the re-sampling factor $factor$ in order to obtain the same number of observations N in each curve; $\{(\hat{x}(k), \hat{y}(k))\}_{k=1}^N$ is the obtained dataset.
- 6: Normalization: resistance and reactance curves extracted from the 1st dataset are divided by the magnitude:

$$\{(x(k), y(k))\}_{k=1}^N = \left\{ \frac{(\hat{x}(k), \hat{y}(k))}{\max_{k \in \{1, \dots, N\}} \sqrt{\hat{x}^2(k) + \hat{y}^2(k)}} \right\}_{k=1}^N$$

- 7: Extraction of dynamical system parameters vectors (θ_x, θ_y) from $\{(x(k), y(k))\}_{k=1}^N$ and the Recursive Least Squares algorithm:

- set the forgetting factor $\alpha \in [0, 1]$, the value σ for the initial auto-correlation matrix of data $P(0) = \sigma I$, and $(\theta_x(0), \theta_y(0))$ the initial parameters vectors
- **for** $i \in \{1, \dots, N\}$ **do**
 $\xi_x(k) \leftarrow x(k) - \theta_x^T(k-1)\phi_x(k)$,
 $\theta_x(k) \leftarrow \theta_x(k-1) + \frac{\xi_x(k)P(k-1)\phi_x(k)}{\alpha + \phi_x(k)^T P(k-1)\phi_x(k)}$,
 $P(k) \leftarrow \frac{P(k-1)}{\alpha} \left[I - \frac{\phi_x(k)\phi_x(k)^T P(k-1)}{\alpha + \phi_x(k)P(k-1)^T \phi_x(k)} \right]$
- **end for**

- 8: Using a multi-class Support Vector Machines for determining angle:

- set θ the concatenation of θ_x and θ_y
- the dataset of θ is separated in two parts. the first part will be used for training and the second part for evaluation algorithm performance
- set the kernel, the kernel parameter and the positive constant of tolerance C

- 9: Using a multi-class Support Vector Machines and the 2nd dataset $\{(\hat{x}(k), \hat{y}(k))\}_{k=1}^M$ for determining the depth among depths belonging to the previously found angle group:

- calculation of the magnitude mg :

$$mg = \max_{k \in \{1, \dots, M\}} \sqrt{\hat{x}^2(k) + \hat{y}^2(k)}$$

- the subset of the 2nd dataset containing magnitudes of the previously found angle is used for training and the second part of data used in step 8 is used for the evaluation
 - set the kernel, the kernel parameter and the positive constant of tolerance C
-

²Free available on the website: <http://wireless.feld.cvut.cz/diagnolab/node/16>

quality of extracted feature so that this one could be used to the second step. The assumption is that whatever the type of crack, the used model structure is fixed. Then, only the parameter of the identified model will be used to characterize the type of crack.

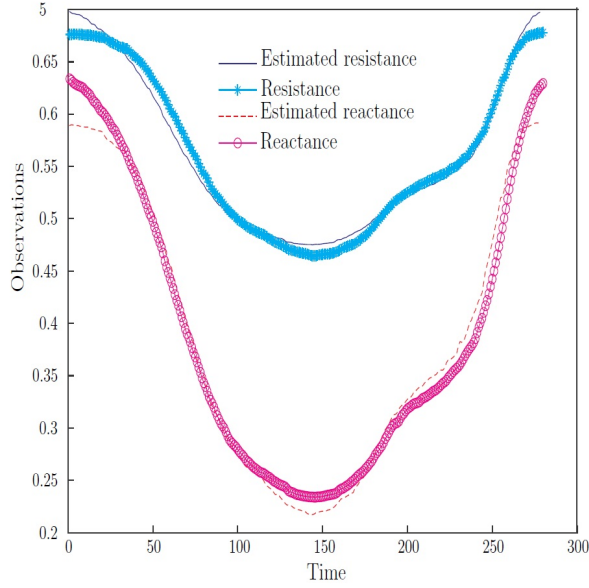


Figure 4. Estimation of resistance and reactance from two order dynamical systems model.

For each crack data recorded, the pair of extracted parameters vectors (θ_x, θ_y) belongs to $\mathbb{R}^3 \times \mathbb{R}^3$. Figures 5 and 6 show these parameters in two three-dimensional spaces. It can be seen that the four groups are well separated. Before classifying, parameters θ_x and θ_y are concatenated. The new vector from this concatenation θ belongs to \mathbb{R}^6 .

The One Against One SVM with a Gaussian kernel is used for the classification. The pair (σ, C) of the kernel parameter and the constant of tolerance are searched into a grid $[10^{-5}, 10^4] \times [10^{-5}, 10^4]$ containing 100 equidistant pairs. The selected pair $(\sigma = 10, C = 10)$ is that minimizes the miss-classification error rate after using leave-one-out cross validation. The minimum of the miss-classification error rate is equal to 1.25%. Tables 1 shows the confusion matrix of the One Against One SVM. Thus, we can say that our approach has a good classification performance with respect to the penetration angle into material.

In order to evaluate the efficiency of our classification procedure, we are going to realize the classification with extracted parameters obtained by a Principal Component Analysis applied on Fourier descriptors (FD-PCA). The FD-PCA procedure consists firstly to extracted Fourier descriptors from our crack observations. Discrete Fourier descriptors are defined

as

$$df(p) = \frac{1}{N} \sum_{k=1}^N z(k) \exp(-j2\pi p(k-1)/N), p = 1, \dots, N$$

After the calculation of the discrete Fourier descriptors for each crack observation, the most representative descriptors are selected by using Principal Component Analysis. Three complex descriptors are chosen and these ones represent 93% of the total variance. By using One Against One SVM and the leave-one-out cross validation, the miss-classification error rate is equal to 7.5%. Tables 2 shows the confusion matrix of the classification based on the FD-PCA procedure.

It can be seen that our extraction procedure based on dynamical systems combined to SVM gives better results than the FD-PCA procedure combined to SVM for the same number of extracted parameters (6 real parameters for the first one and 3 complex parameters for the second one). Thus, our classification algorithm is efficiency and promising.

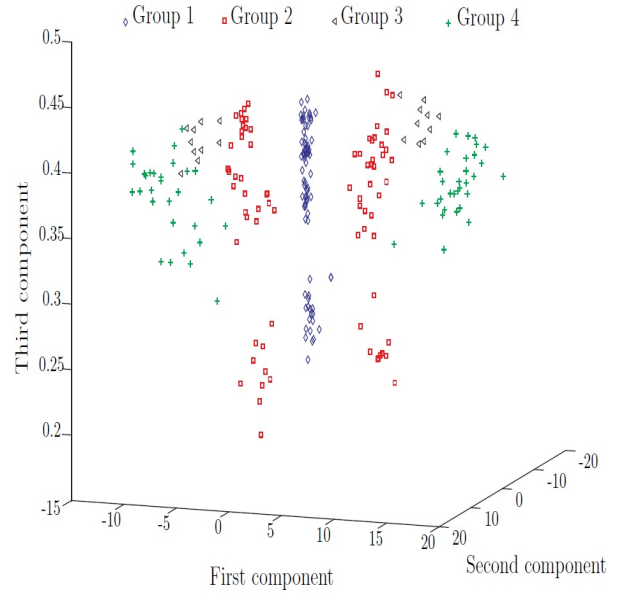


Figure 5. Illustration of the parameter θ_x for the four crack groups.

Table 1. Confusion matrix of the One Against One SVM.

Actual Group	Predicted Group			
	Group 1	Group 2	Group 3	Group 4
Group 1	80	0	0	0
Group 2	0	80	0	0
Group 3	0	0	19	1
Group 4	0	1	1	58

The second step of classification consists of discriminating the penetration depth for cracks with the same penetration

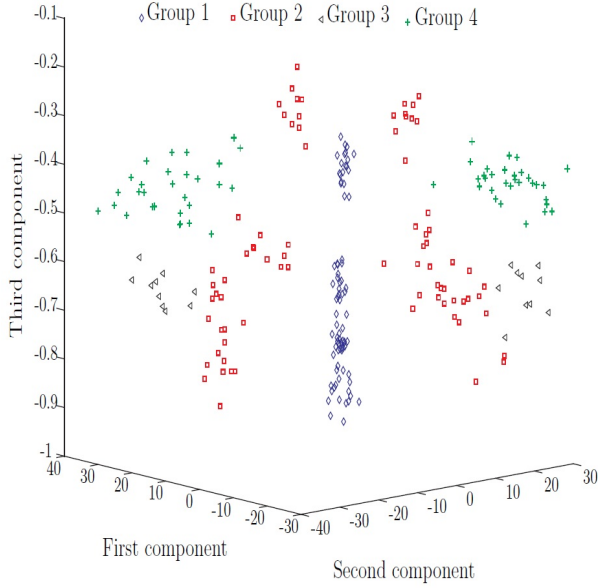


Figure 6. Illustration of the parameters θ_y for the four crack groups.

Table 2. Confusion matrix of the One Against One SVM applied on the FD-PCA feature extraction.

Actual Group	Predicted Group			
	Group 1	Group 2	Group 3	Group 4
Group 1	77	3	0	0
Group 2	8	71	1	0
Group 3	0	2	17	1
Group 4	0	1	2	57

angle. To do this, the second dataset, i.e., without normalization is used. Figure 7 shows the second classification step in group 1. Similar figures are obtained for groups 2 and 4. For cracks classified in group 3, there is not a second step because the penetration depth is unique (1.5mm). According to this figure, recorded data can be well separated by hyperplanes. The One Against One SVM with a Gaussian kernel is used for the three classifications in the second step. As we previously mentioned, the pair (σ, C) of the kernel parameter and the constant of tolerance are searched into a grid $[10^{-5}, 10^4] \times [10^{-5}, 10^4]$ containing 100 equidistant pairs. The selected pairs of kernel parameter and constant of tolerance of group 1, 2 and 4 are respectively $(\sigma = 1, C = 1)$, $(\sigma = 0.1, C = 0.1)$ and $(\sigma = 0.1, C = 0.1)$. The miss-classification error in step two, i.e. for the three classifications is null. In other words, according to available data, if a crack is classified in the right group (ie, if the right angle is selected), the right depth is automatically selected. Hence, the global miss-classification error is equal to the first step miss-classification (approximately equal to 1%).

Remark.

The previous classification uses Gaussian kernel. However, when Gaussian kernel is replaced by homogenous polynomial kernel respectively with parameters $(d = 3, C = 10^{-3})$, the same miss-classification error is obtained. Our classification seems robust with respect to the selected SVM kernel.

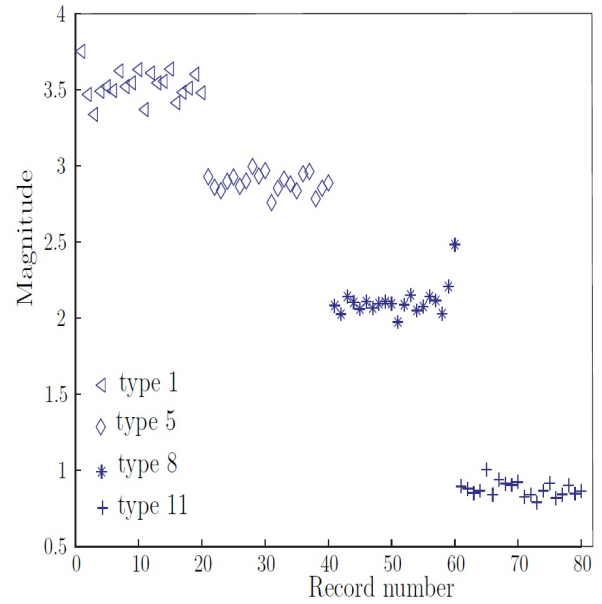


Figure 7. Impedance magnitude of the first group records.

7. CONCLUSION

This paper addresses the problem of classifying cracks by using measurements of Eddy currents. The paper proposes a new approach for cracks classification which uses dynamical systems. The parameters of these dynamical systems form the feature space. The parameters vectors are found from the measured data by using an algorithm from systems identification. The classification is done in two steps. The first one is to group cracks according to their penetration angles into the material. The second one is to group them according to penetration depths. Our method is evaluated on a particularly challenging benchmark, for which the cracks are more difficult to classify due to the variation of the scanning speed. After using multi-class SVM for both steps classification, the miss-classification error is approximately equal to 1%. This means that our approach is efficiency and promising.

REFERENCES

Cantrell, J. H., & Yost, W. T. (2001). Nonlinear ultrasonic characterization of fatigue microstructures. *Interna-*

- tional Journal of Fatigue*, 23, Supplement 1(0), 487 - 490.
- Caruana, R., & Niculescu-Mizil, A. (2006). An empirical comparison of supervised learning algorithms. In *Proceedings of the 23rd international conference on machine learning* (pp. 161–168). New York, NY, USA: ACM. doi: 10.1145/1143844.1143865
- Clark, M., McCann, D., & Forde, M. (2003). Application of infrared thermography to the non-destructive testing of concrete and masonry bridges. *Ndt & E International*, 36(4), 265–275.
- Elaqra, H., Godin, N., Peix, G., R'Mili, M., & Fantozzi, G. (2007). Damage evolution analysis in mortar, during compressive loading using acoustic emission and x-ray tomography: Effects of the sand/cement ratio. *Cement and Concrete Research*, 37(5), 703 - 713.
- Jie, L., Siwei, L., Qingyong, L., Hanqing, Z., & Shengwei, R. (2009, July). Real-time rail head surface defect detection: A geometrical approach. In *Industrial electronics, 2009. isie 2009. ieee international symposium on* (p. 769-774).
- Jo, N. H., & Lee, H.-B. (2009). A novel feature extraction for eddy current testing of steam generator tubes. *{NDT} & E International*, 42(7), 658 - 663.
- Khelil, M., Boudraa, M., Kechida, A., & Draï, R. (2005). Classification of defects by the svm method and the principal component analysis (pca). *World Acad. Sci. Eng. Technol*, 9, 226–231.
- Lingvall, F., & Stepinski, T. (2000). Automatic detecting and classifying defects during eddy current inspection of riveted lap-joints. *{NDT} & E International*, 33(1), 47 - 55.
- Liu, B., Hou, D., Huang, P., Liu, B., Tang, H., Zhang, W., ... Zhang, G. (2013). An improved pso-svm model for online recognition defects in eddy current testing. *Non-destructive Testing and Evaluation*, 28(4), 367-385.
- Ljung, L., & Söderström, T. (1983). *Theory and practice of recursive identification*. MIT press Cambridge, MA.
- Madaras, E. I., Prosser, W. H., & Gorman, M. R. (2005). Detection of impact damage on space shuttle structures using acoustic emission. In *Review of progress in quantitative nondestructive evaluation: Volume 24* (Vol. 760, pp. 1113–1120).
- Mercer, J. (1909). Functions of positive and negative type, and their connection with the theory of integral equations. *Philosophical Transactions of the Royal Society, London*, 209, 415–446.
- Moreira, M., & Mayoraz, E. (1998). Improved pairwise coupling classification with correcting classifiers. In *Machine learning: Ecml-98* (pp. 160–171). Springer.
- Němec, H., Kužel, P., Garet, F., & Duvillaret, L. (2004). Time-domain terahertz study of defect formation in one-dimensional photonic crystals. *Applied optics*, 43(9), 1965–1970.
- Oukhellou, L., Aknin, P., & Perrin, J.-P. (1999). Dedicated sensor and classifier of rail head defects. *Control Engineering Practice*, 7(1), 57 - 61.
- Smid, R., Docekal, A., & Kreidl, M. (2005). Automated classification of eddy current signatures during manual inspection. *NDT & E International*, 38(6), 462–470.
- Song, S.-J., & Shin, Y.-K. (2000). Eddy current flaw characterization in tubes by neural networks and finite element modeling. *{NDT} & E International*, 33(4), 233 - 243.
- Vapnik, V. (2000). *The nature of statistical learning theory*. Springer.
- Ye, B., Huang, P., Fan, M., Gong, X., Hou, D., Zhang, G., & Zhou, Z. (2009). Automatic classification of eddy current signals based on kernel methods. *Nondestructive Testing and Evaluation*, 24(1-2), 19–37.